CHALMERS
UNIVERSITY OF TECHNOLOGY

Induced effects on cables laid in the vicinity of substation lightning masts

Master's thesis in Electric Power Engineering

ANTON ERIKSSON

Department of Electrical Engineering
CHALMERS UNIVERSITY OF TECHNOLOGY
Gothenburg, Sweden 2020

Master's thesis

Induced effects on cables laid in the vicinity of substation lightning masts

ANTON ERIKSSON

CHALMERS
UNIVERSITY OF TECHNOLOGY

Department of Electrical Engineering
Division of Electric Power Engineering
Chalmers University of Technology
Gothenburg, Sweden 2020

Induced effects on cables laid in the vicinity of substation lightning masts
Anton Eriksson

Supervisor: Joan Hernandez, Senior Project Engineer, ABB Power Grids
Examiner: Prof. Yuriy Serdyuk, Department of Electrical Engineering

Master's Thesis
Department of Electrical Engineering
Division of Electric Power Engineering
Chalmers University of Technology
SE-412 96 Gothenburg
Telephone +46 31 772 1000

Typeset in LaTeX
Gothenburg, Sweden 2020

Induced effects on cables laid in the vicinity of substation lightning masts
Anton Eriksson
Department of Electrical Engineering
Chalmers University of Technology

Abstract

The disturbances induced in low voltage cables in an HVDC substation during a lightning strike to a mast were evaluated using the simulation tool HIFREQ. To analyse the observed effects, an equivalent circuit approach was utilised and a model of a simplified cable was developed and implemented in Simulink. A set of simulations was conducted to study the origins of the disturbances. The result shows that the main reason for the disturbance was the high ground potential difference between cable screen grounding points created during lightning, which caused a screen current to flow.

The magnitudes of the disturbances were found to be below 90 V per kA of the lightning current for all the simulated cables. Different mitigation methods (adding parallel conductors to the cable, changing configuration of the mast, etc.) were tested to evaluate their effectiveness in damping the disturbances. Moreover, a risk analysis based on the rolling sphere method was conducted to investigate how often faults in low voltage cables can be expected. It was concluded that the risk of cable breakdown is negligible in comparison to the risk of cable overheating due to the high screen current.

Keywords: Ground Potential Rise, Grounding, Cable Lightning Disturbance, Lightning protection, Rolling Sphere Method, CDEGS, HIFREQ, HVDC.

Acknowledgements

Firstly I would like to thank my supervisor at ABB Power Grids, Joan Hernandez, and everybody at the TSC department of ABB Power Grids who has guided and helped me with my work. I would also like to acknowledge the CDEGS support team who provided me with good technical guidance for problems that have occurred with the simulations in HIFREQ. Lastly I would like to thank my examiner, Yuriy Serdyuk, for always taking time to answer my questions and providing useful comments on the work.

Anton Eriksson, Gothenburg, May, 2020

Contents

List of Figures

List of Tables

Acronyms

CDEGS Current Distribution, Electromagnetic Interference, Grounding and Soil Structure Analysis, Earthing Software. 19, 43
CG Cloud to Ground. 13

GPD Ground Potential Difference. xi, 5, 11, 31–33, 43
GPR Ground Potential Rise. 2, 5–7, 11, 20

HVDC High Voltage Direct Current. xi, 1–3, 19, 20, 43

LCC Line Commutated Converters. 1
LV Low Voltage. 2, 7, 8, 28, 41

PEC Parallel Earthing Conductor. xi, 10, 21, 22, 24, 26, 27, 33, 34, 37–41, 43

VSC Voltage Source Converters. xi, 1–3, 20

1
Introduction

1.1 Problem description and background

High Voltage Direct Current (HVDC) technology has characteristics that make it especially attractive for certain transmission applications. It is widely recognised as being advantageous for long-distance bulk-power delivery, asynchronous interconnections, and long submarine cable crossings.

HVDC technology can be split into two different branches depending on the converter type used. One relies on thyristor based Line Commutated Converters (LCC) for the conversion between AC and DC and the other uses IGBT Voltage Source Converters (VSC). VSC-HVDC is typically used for connections with lower voltage and power rating and comes with certain benefits that LCC-HVDC can not provide. Such as being able to assist in the black start of an AC grid and provide reactive power compensation.

A VSC-HVDC station also has a much smaller footprint compared to a LCC-HVDC station. The layout of a typical VSC-HVDC station is shown in Figure 1.1.

Figure 1.1: An VSC-HVDC station [1].

The VSC semiconductor valves are placed inside buildings, and DC and AC yards can be in buildings on request. Lightning masts are placed in the converter sta-

tion to protect the equipment from lightning. Low voltage power and signals cables are routed from the control and auxiliary building to the different equipment in the station. As a result of the smaller footprint, Low Voltage (LV) cables need to be routed closer to lightning masts in VSC-HVDC stations. Lightning strokes to masts produce travelling waves along the mast and grounding grid which is a common source of electromagnetic disturbances to cables. The Ground Potential Rise (GPR) associated with a lightning strike also contribute to cable disturbances.

Previous work on computational simulations of lightning disturbances to cables has been done, mainly focusing on railway systems [5] and small substations using single core cables [6]. The main shortcomings of applying the previous work on HVDC converter stations are that they have not included cables with multiple core conductors and the specific connections at the cable terminations are not discussed. Also, the risk of the overvoltages damaging the cable has not been investigated and only a limited number of mitigation methods have been evaluated.

1.2 Aim

The aims of this thesis are to:

i Perform a technical review of electrical disturbances to LV cables caused by lightning strikes to neighbouring structures.

ii Identify the main parameters affecting cable disturbances, create simulation models to reproduce the effects in order to evaluate the magnitude of the disturbances.

iii Propose and validate mitigation methods that permit routing cables beneath lightning masts.

iv Perform a risk analysis for the proposed mitigation methods.

1.3 Scope

To reduce the number of cases to simulate, only negative downward lightning was analysed as this accounts for the vast majority of substation lightning [7]. Further more, only primary lightning strokes were simulated as subsequent strokes tend to be of much lower current and energy [4].

Only the temperature and voltage rating of cables were considered for the risk analysis. The damage to equipment connected to the cables were not considered as these might have other voltage and current ratings.

1.4 Societal and environmental aspects

Most countries aim to reduce their dependency on non renewable energy sources for electricity production to mitigate climate change. HVDC has several characteristics that can play a vital part in completing this energy transition in a successful

way. VSC-HVDC is commonly used to connect offshore wind farms to the mainland as it is efficient in long submarine connections. Also, the long distance power transmission that HVDC provides can be used to incorporate untapped renewable energy resources located far from large cities to the power system. An area with high transmission capabilities will also be more resilient to weather fluctuations as it can more easily export energy when the weather is favourable and import when the production is low.

Another aspect of HVDC are the societal benefits. HVDC can in many cases offer a cost effective solution for grid investments. Which can result in lower transmission costs for the consumers. The high power transfer capability of HVDC can also reduce the number of power lines needed in comparison to traditional AC power transmission. This implies that less land needs to be occupied by power lines and can be used for other purposes.

As the aims of this thesis are related to improving the reliability of HVDC stations and reducing cost and size. The result could help in making HVDC technology a more viable option for new transmission grid investments. Decreasing the time for countries to transition into more renewable energy production and reducing the cost. This thesis investigates VSC-HVDC stations but the principals discussed apply to both AC and HVDC substations where cables need to be routed close to lightning masts.

2

Cable disturbances during lightning

2.1 Station grounding system

The grounding system is an important part of an electrical station as it provides a low impedance path to ground for fault and lightning currents, which reduces the GPR of the station. A high GPR can be dangerous for humans as it implies high step and touch voltages and can cause flashovers between points with a high Ground Potential Difference (GPD) [8]. The GPD between different points in the station can also result in high currents flowing in metallic objects grounded at multiple points in a station.

A substation grounding system is often composed of a grounding grid and grounding rods. The grid consists of bare conductors, buried underground and extends over the entire substation. A grounding rod is a bare conductor extending downward, into the soil. The grounding resistance is affected by many parameters, e.g. the mesh size of the grounding grid, the number of grounding rods and the soil resistivity. Smaller grid meshes and grounding rods will result in a lower grounding resistance [8]. Therefore, substations placed in regions with a high soil resistivity tend to uses smaller grid meshes and more grounding rods.

2.1.1 Soil parameters

Soil resistivity and permitivity are important parameters affecting the GPR of a station during a lightning strike. A low soil resistivity implies a low GPR since the current can easily disperse into the soil. A high soil permitivity will contribute to capacitive effects in the soil, reducing the soil impedance at higher frequencies and therefore decrease the GPR of the station. The soil resistivity is the lowest for wet soil, with a value in the range of 10 Ω·m. Dry soil has a resistivity around 1000 Ω·m and bedrock 10 000 Ω·m [8]. The soil relative permitivity varies between approximately 4 for dry soil and 20 for wet soil. However, both the electrical resistivity and permittivity has some frequency dependency and tend to decrease with increasing frequencies [9]. When a material is energised by an electric field, a current will flow with a current density equal to

$$\mathbf{J_{Tot}} = \mathbf{J_C} + \mathbf{J_D} = \sigma_0 \mathbf{E} + j\omega\epsilon\mathbf{E}, \tag{2.1}$$

where J_C is the conduction current, J_D the displacement current, σ_0 the DC conductivity and ϵ the permitivity. ϵ is a complex number equal to $\epsilon = \epsilon' - j\epsilon''$ which implies

$$\mathbf{J_{Tot}} = \sigma_0\mathbf{E} + j\omega(\epsilon' - j\epsilon'')\mathbf{E} = (\sigma_0 + \omega\epsilon'')\mathbf{E} + j\omega\epsilon'\mathbf{E}. \tag{2.2}$$

The real part of the permittivity is related to the materials polarization and energy storage ability. The imaginary part is related to the losses during the polarization of the material. The permittivity generally decrease with increasing frequency since the slower polarization processes with higher inertia does not have time to get polarised during one cycle of the fast changing field. Implying less polarisation per cycle and thus a lower value of ϵ'. The conductivity $\sigma = \sigma_0 + \omega\epsilon''$ increase with increasing frequency and thus the resistivity decrease. The GPR caused by a lightning strike is largely dependant on the soil resistivity and thus not taking into account to frequency dependency of soil parameters could lead to an overestimation of the GPR. The soil permittivity is related to the capacitive effect of the soil. Increasing the permittivity implies a higher capacitance and thus a lower soil impedance [10].

It has been suggested that the frequency dependency of the soil resistivity and permitivity should be modelled as

$$\rho = \frac{\rho_0}{1 + 0.47 \cdot 10^{-6}\rho_0^{0.73} f^{0.54}}, \tag{2.3a}$$

$$\epsilon = 9.5 \cdot 10^4 \rho_0^{-0.27} f^{-0.46} + 12, \tag{2.3b}$$

where ρ_0 is the DC soil resistivity [9].

Another aspect to consider when modelling the electrical characteristics of soil is ionisation. When lightning strikes a structure, the surrounding soil will experience a strong electric field. In the region where the electric field strength exceeds the breakdown strength of the soil, the soil will get ionised and the resistivity will decrease drastically [11]. This can be seen as increasing the size of the grounding electrode since the surrounding soil becomes conducting and the GPR associated with the lightning strike is then decreased. The breakdown strength of soil tend to vary greatly depending on soil type and decrease with increasing moisture content. However, the breakdown strength is always lower than that of air and it has been suggested that the breakdown strength varies between 300 to 400 kV/m [12].

2.2 Cable disturbances

2.2.1 Lightning disturbances

When a lightning strikes a mast in a substation, a high GPR is generated in the surrounding area. During the first micro seconds of the strike, the increase in current is very steep and therefore the lightning impulse contains high frequencies. The impedance of the grounding grid for the high frequency part of the impulse increase significantly due to the grid's inductance. This implies that more current will flow through the soil, creating a high GPR close to the lightning mast which quickly decrease when moving away from the tower. As the steep front of the impulse is over, only the low frequency part of the impulse remains and the impedance of the grid decrease. This implies that less current will flow in the soil and the GPR of the grid becomes approximately uniform [13].

The screen of a LV cable in the station, which is grounded at different points of the grid, will experience a high potential difference between it's two ends (during the first micro seconds) if one point is grounded close to the mast. The potential difference will consist of two components, the GPR difference between the two grounding points and the induced component due to the mutual inductance between the screen and the grounding grid. The two components are of opposite sign and the GPR difference is the dominant one if the cable is grounded close to the mast [6].

The potential difference will give rise to a current in the screen which is coupled to a potential difference between the cable screen and core conductors though the transfer impedance of the cable [14]. The equivalent circuit of a short cable segment with one core conductor of the length Δl is shown in Figure 2.1.

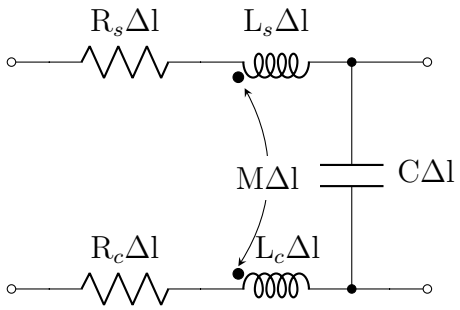

Figure 2.1: Equivalent circuit of a short cable segment [2].

Where R_s and L_s are the screen parameters, R_c and L_c the core parameters and C the capacitance between the screen and core. The high frequency component of the screen current will be shared between the screen and core conductor due to the capacitance of the cable, which presents a lower impedance as the frequency increase. When current flows through a capacitor, a voltage is created according to

$$V(t_1) = \frac{1}{C}\int_{t_0}^{t_1} I_C \, dt + V(t_0), \tag{2.4}$$

where C is the capacitance, I_C the current and V(t) the voltage. From this reasoning it can be concluded that if the frequency content or magnitude of the screen current is increased, more current will flow to the core conductor and the voltage disturbance will increase.

There is also a mutual inductance between the screen and the core conductor [14]. Current flowing in the screen will induce a current of opposite direction in the core conductor to reduce the created magnetic field. The induced current will be of opposite sign to the capacitive current and thus the induction will mitigate the disturbance. As the cable can be seen as a series of RLC networks, the core current and core to screen voltage will contain oscillations if the lightning current contains the cables oscillation frequency.

2.2.2 Rated impulse voltage

Low voltage power and signal cables rated below 3 kV are not subjected to impulse tests and are only tested under steady state conditions according to IEC standards [15]. Solid insulation can, however, withstand much higher impulse voltages compared to steady state AC voltages [16]. The dielectric strength of typical polyethylene (PE) and cross linked polyethylene (XLPE) insulation used in LV cables is between 35-50 kV/mm [17].

2.2.3 Cable parameters

When considering high frequency cable disturbances, which occurs during a lightning strike, the frequency dependency of parameters such as the resistance and inductance should be included. For a coaxial cable with a solid inner conductor, the DC resistance can be calculated as

$$R_{DC,Inner} = l\frac{\rho}{\pi r^2}, \tag{2.5a}$$

$$R_{DC,Screen} = l\frac{\rho}{\pi(r_2^2 - r_1^2)}, \tag{2.5b}$$

where l is the length of the cable, ρ the conductor resistivity, r the inner conductor radius, r_1 the inner screen radius and r_2 the outer screen radius. However, when a high frequency current flows through the cable, the current will be pushed out from the middle of the conductor. This phenomenon is known as the skin effect and is caused by induced eddy currents cancelling out the current in the middle of the conductor and increasing the current close to the conductors surface. This will cause current to only flow in a region between the outer surface of the conductor and a certain skin depth [18]. The skin depth and the resulting resistance (assuming that the skin depth is shorter than the conductor radius or screen thickness) can be

calculated as

$$\delta = \sqrt{\frac{2\rho}{\omega\mu}} \implies R_{AC} = l\frac{\rho}{\pi(r^2 - (r^2 - \sqrt{\frac{2\rho}{\omega\mu}})^2)}, \tag{2.6}$$

where ω is the angular frequency, μ the permeability of the conductor and r the radius of the conductor (outer radius if calculated for the screen).

The conventional way of calculating the inductance of a cable with coaxial geometry is to assume that all the current flowing in the core returns through the screen. Which cancels out the magnetic field outside of the cable. However, this is not the case when considering lightning disturbance to a cable as the screen current will dissipate in the soil instead of returning through the core. Instead, the core and screen inductance must be separated. The low frequency per meter self inductance of a straight wire can be calculated as

$$L_{Self} = \frac{\mu_r\mu_0}{2\pi}(\ln(2l/r) - 0.75), \tag{2.7}$$

where μ_0 is the permeability of free space and μ_r the relative permeability [19]. Part of this inductance comes from the magnetic field inside the wire, called the internal inductance. At high frequencies, the current will only flow at the conductors outer boundary and thus the inner inductance will tend to zero and needs to be subtracted. The inner inductance is given by $L_{inner} = \frac{\mu}{8\pi}$ [19]. This is also true for a thin hollow cylinder (screen) as the inner inductance is small and needs to be subtracted, resulting in

$$L_{Self} = \frac{\mu}{2\pi}(\ln(2l/r) - 0.75) - \frac{\mu}{8\pi} = \frac{\mu}{2\pi}(\ln(2l/r) - 1). \tag{2.8}$$

The mutual inductance between the screen and core is equal to the screen inductance as all of the magnetic flux produced by a current flowing in the screen encompasses the core conductor [14]. The capacitance of a coaxial cable in not dependant of the skin effect, however, as discussed in 2.1.1, polarization of the insulation will be affected at higher frequencies and the permittivity will decrease. If the frequency dependency of the insulation permittivity is neglected, the capacitance per meter of a coaxial cable can be calculated as

$$C = \frac{2\pi\epsilon_r\epsilon_0}{\ln(\frac{r_s}{r_c})}, \tag{2.9}$$

where ϵ_0 is the permittivity of free space, ϵ_r the relative permittivity of the insulation material, r_s the inner radius of the screen and r_c the radius of the core [18].

2.2.4 Heating of cables

During a lightning strike, conductors close to the striking point will conduct a high portion of the lightning current which can result in a significant conductor temperature increase. As lightning is a phenomenon with a very short duration, almost no heat will be removed from the conductor during the strike and the heating process can be seen as adiabatic [3]. The heating energy absorbed by a conductor subjected to a current impulse can be calculated as

$$W = R \int_0^T i(t)^2 dt, \tag{2.10}$$

where R is the resistance of the conductor, i(t) is the current flowing in the conductor and T the duration of the current impulse. For an adiabatic process the temperature increase of a conductor can be calculated as

$$\Delta\theta = \frac{1}{\alpha}\left(exp\left(\frac{\frac{W}{R}\alpha\rho}{q^2\gamma C_W}\right) - 1\right), \tag{2.11}$$

where $\Delta\theta$ is the temperature increase of the conductor, α the resistance temperature coefficient, $\frac{W}{R}$ the energy of the impulse divided by the resistance, ρ the conductor resistiviy at ambient temperature, q the cross section area , γ the density and C_W the thermal capacity [3]. The parameter values for copper is shown in Table 2.1.

Table 2.1: Material parameters for copper used in equation 2.11 [3].

Parameter	Copper
α	$3.92{\cdot}10^{-3}$ K^{-1}
ρ	$17.8{\cdot}10^{-9}$ Ωm
γ	8920 kg/m^3
C_W	385 J/kgK

The rated short circuit temperature of PE insulation is 130 °C and 250 °C for XLPE insulation [17].

2.2.5 Mitigation methods

There are multiple methods used to mitigate cable disturbances during a lightning strike. Adding parallel conductors close to the cable, such as Parallel Earthing Conductor (PEC) and cable ladders, connected to the grounding grid at multiple points is one method commonly used. Having a grounded conductor close to a cable will provide another path for the lightning current to flow, reducing the screen current [13]. The mutual inductance between the added conductor and screen will further reduce the screen current. The same effect can be achieved by having cables routed close to each other, as this increases the mutual inductance between the cable screens.

Another mitigation method is to move the connection point between the mast and the grounding grid away from cable grounding points. This would reduce the GPD between cable grounding points which reduces the screen current. However, as the conductor length between the top of the mast and the connection point increase, so does the inductance which increases the GPR of the mast during a lightning strike.

3

Lightning characteristics

Lightning is the result of charge formation in clouds and can occur within clouds or from Cloud to Ground (CG) where lightning within clouds is the most common and account for approximately 75 % of all lightning [20]. Since only CG lightning is associated with substation disturbances, this type of lightning is considered in lightning protection systems. There are four different types of CG lightning [4]:

- Positive upward flashes
- Negative upward flashes
- Positive downward flashes
- Negative downward flashes

Upward flashes are initiated from ground, going up to the charged cloud and downward flashes are initiated from the cloud, striking downwards to the ground. Upward flashes are most common for tall structures (above 60-100 m) and generally does not occur in substation [7], [20]. Thus only positive and negative downward flashes are considered in substation lightning protection. The polarity of the flash refers to the polarity of the cloud. Meaning a lightning current going towards the cloud for negative downward flashes and towards ground for positive downward flashes. Approximately 10 % or less of all downward flashes are positive and the remaining 90 % negative [7], [21].

The lightning current pulse shape varies greatly between each individual flash. But for lightning impulses, which generally have a duration shorter than 2 ms, the pulse shape can be approximated according to Figure 3.1

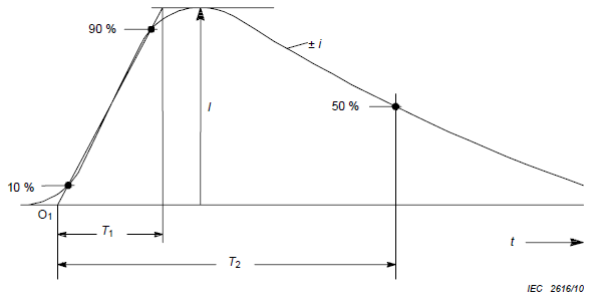

Figure 3.1: Lightning current impulse shape and parameters [3].[1]

Where T_1 is the front time, T_2 the time to half, I the peak current and O_1 the virtual origin. IEC recommends the use of the Heidler function to approximate the

[1] IEC 62305-1 ed.2.0 "Copyright © 2010 IEC Geneva, Switzerland. www.iec.ch"

lightning current pulse shape according to

$$I(t) = I_m \frac{1}{\eta} \frac{(\frac{t}{\tau_1})^n}{1 + (\frac{t}{\tau_1})^n} e^{-t/\tau_2}, \tag{3.1}$$

where I_m is the peak current, τ_1 and τ_2 time constants associated with the rise and fall time of the impulse, η a constant to adjust the amplitude and n a constant set to 10 [3].

The main reason behind cable disturbance is the current steepness ($\frac{di}{dt}$) and thus the Lightning parameters of interest are peak current and front time [3]. The peak current can be approximated to have a log normal cumulative distribution. The statistical distributions (probability that the peak current of a lightning strike will exceed a certain current) of the negative downward lightning peak current is show in Figure 3.2.

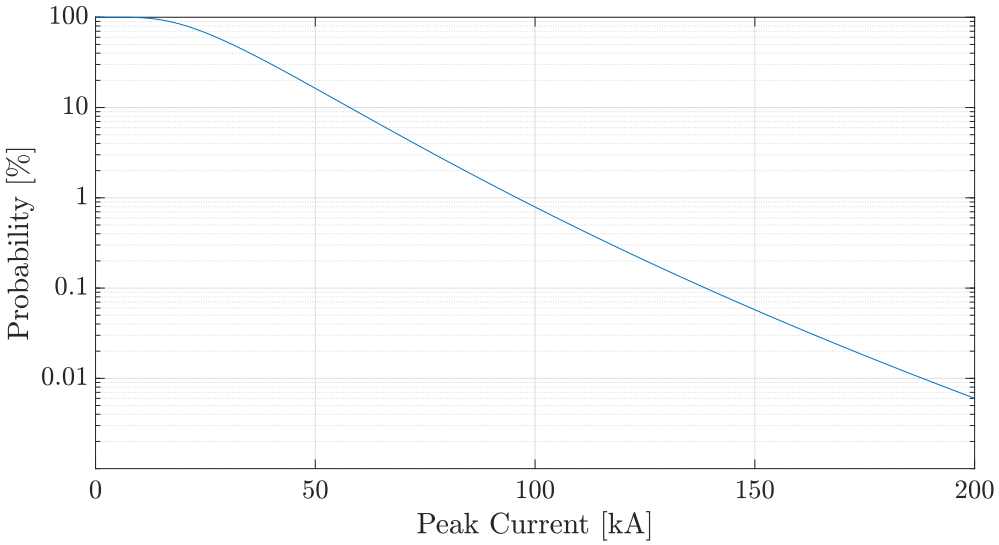

Figure 3.2: Log normal cumulative distribution function (probability that the peak current exceeds a given current) using β=0.484 and a mean current of 31.1 kA.

Positive downward flashes generally have a higher peak current compared to negative flashes, but negative downward flashes has a shorter front time [4]. Subsequent negative strokes have the lowest peak current but the shortest front time and thus the highest frequency content. Positive following strokes are uncommon and only account for about 10 % of all positive lightning. This implies that there is a limited amount of data on the characteristic of positive following strokes [7]. The suggested median values for the peak currents and front times are shown in Table 3.1

Table 3.1: Median peak current and front time for different lightning types [4].

Lightning type	I_m [kA]	T_1 [μs]
Negative first stroke	30	5.5
Negative subsequent stroke	12	1.1
Positive first stroke	35	22

The peak current and front time has a low correlation [20]. In [4] it was determined that the correlation coefficient is 0.36 and thus the two parameters can be seen as independent for engineering applications. In [3] it is recommended to use a front time of 1 µs for analysis of negative first strokes, which is considerably lower than the median value. This is probably recommended so that tests are done for the worst case scenario with a short front time and high ($\frac{di}{dt}$). As the time to half is not of great importance to the front steepness, its value is of less importance for the voltage disturbance but it can be important when considering temperature rise of conductors, 200 µs is recommended for analysis [3].

3.1 Lightning strikes to grounded structures

3.1.1 Ground flash density

The ground flash density (number of cloud to ground lightning strikes per unit time-area) varies greatly across the globe. Generally it is higher close to the equator and lower close to the poles. The ground flash density can be approximated according to

$$N_g = 0.04\ T_d^{1.25}, \tag{3.2}$$

where T_d is the number of thunderstorm days/year [7]. T_d tend to be below 10 days/year in northern Europe and can reach values above 30 days/year in southern Europe. In certain regions near the equator, T_d has been measured to above 200 days/year [22]. Some locations also measure the ground flash density directly by documenting all lightning strikes. In the US for example, the maximum ground flash density was measured to over 12 flashes/km^2/year in 2018 [23].

3.1.2 Rolling sphere method

The rolling sphere method can be used to approximate the protection zone in the proximity of a lightning mast. It is based on the electrogeometric model, which assumes that the formation of the flash will propagate in steps, called step leaders. The length of the last stepped leader is known as the striking distance can be

approximated according to

$$S = 10I_s^{0.65}, \tag{3.3}$$

where S is the striking distance and I_s the striking current [22]. Equation 3.3 implies that a lower striking current will have a shorter striking distance. If a lightning strike appears within a distance shorter than or equal to S, it will be attracted to the mast and strike it. However, if the striking distance is greater than the mast height, the attractive radius of the mast will be reduced which can be seen in Figure 3.3.

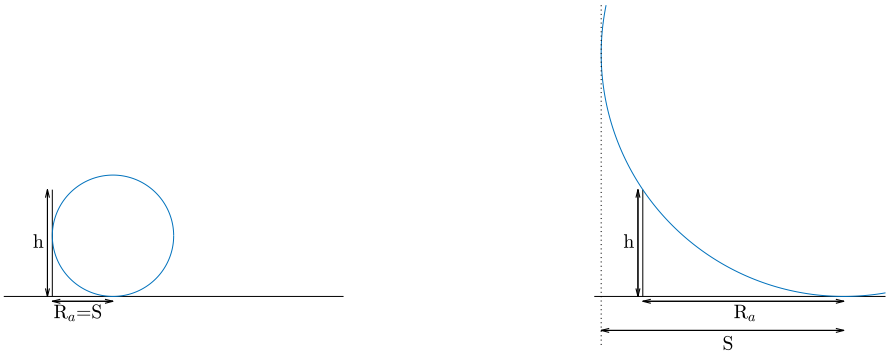

(a) **(b)**

Figure 3.3: The attractive radius of a mast when striking distance is smaller than the mast height (a) and larger than the mast height (b).

Thus the attractive radius of a mast is dependant on the mast height and lightning current and can be calculated as

$$R_a(i) = \begin{cases} S(i) & \text{if} \quad S(i) \leq h, \\ \sqrt{2S(i)h - h^2} & \text{if} \quad S(i) > h, \end{cases} \tag{3.4}$$

where h is the mast height. The number of lightning strikes per year to a mast with no tall structures nearby can be calculated as

$$N_m = N_g A_{eff}, \tag{3.5}$$

where A_{eff} is the effective attractive area of the mast [22]. In a substation there will obviously be other structures and masts near by, but this approximation can be done to simplify the analysis and obtain a slight over approximation of the number of stikes to a mast. The rolling sphere method can be used to calculate the attractive area. The attractive area is dependent on the current, implying that an effective area is needed which takes into account the probability of each lightning current.

With the rolling sphere method, the attractive area can be calculated as

$$A(i) = \pi R_a(i)^2 = \begin{cases} \pi 100 i^{1.3} & \text{if} \quad S(i) \leq h, \\ \pi(2 \cdot 10 i^{0.65} h - h^2) & \text{if} \quad S(i) > h. \end{cases} \tag{3.6}$$

The effective area can be calculated by integrating the probability density function of the current, p(i), times the attractive area as

$$A_{eff} = \int_{i_0}^{\infty} p(i) A(i) di, \tag{3.7}$$

where i_0 can be chosen to zero if all lightning strikes are considered or to the lowest current that cause damage if only the number of damaging strikes are to be calculated. The probability density function can be obtained as

$$p(i) = \frac{1}{\beta i \sqrt{2\pi}} e^{-z^2/2}, \tag{3.8}$$

where

$$z = \frac{\ln(i) - Mean(\ln(i))}{\beta}. \tag{3.9}$$

β is the logarithmic standard deviation of the current and Mean(ln(i)) is the mean value of ln(i). These values can be found in [20] for negative downward flashes, β=0.484 and Mean(ln(i))=ln(31.1). By using the trapz function in matlab, the integral of the effective area can be calculated and then using equation 3.5, the number of strikes per year to a mast can be calculated. The time in between strikes to a mast can be calculated as

$$Y = \frac{1}{N_m}. \tag{3.10}$$

The time between strikes, assuming T_d=10 days/year, for different mast heights is shown in Table 3.2

Table 3.2: Time between strikes to a grounded mast, using T_d=10 days/year, for different mast heights.

Mast height [m]	Time between strikes [yr]
10	250.8
15	172.0
20	132.9
25	109.5
30	94.2

4

Station grounding system and cable simulation setup

The simulation tool HIFREQ was used to investigate the disturbances induced to cables during a lightning strike to an HVDC station. Firstly a simplified cable was examined to investigate environmental factors and mitigation methods. An equivalent circuit of the cable was simulated using Simulink to verify the under lying effect of the cable disturbances. After this, more detailed cables were included in the HIFREQ simulation to investigate the magnitude of the disturbance for a model of a station. The cable types that were included are:

1. Power cable.
2. Signal cable.
3. Current transformer (CT) cable.
4. Lighting cable.

The heating of cables subjected to high lightning currents was also be investigated. Lastly, a risk analysis was conducted to investigate how often faults due to lightning striking the simulated mast can be expected.

4.1 CDEGS simulation tools

Current Distribution, Electromagnetic Interference, Grounding and Soil Structure Analysis, Earthing Software (CDEGS) is an electromagnetic computation software based on the Method of Moments in the frequency domain [24]. It is a powerful software that is commonly used for grounding studies. HIFREQ is a computational module of CDEGS which can be used to simulate both above and underground conductors subjected to high frequency disturbances such as lightning. Both conductive, inductive and capacitive effects between conductors are accounted for in the simulations [25].

A lightning strike to a network of conductors can be simulated by defining a lightning current pulse in the time domain, which is then converted to the frequency domain using the FFTSES computational module. HIFREQ uses the frequency domain data to calculate the current distribution in the conductors. The current distribution is used to calculate the electromagnetic field and potential at selected point in the surrounding space [25]. The result is then converted back to the time domain using FFTSES. The software can detect if there are resonant frequencies is the system and then recommends another run with new frequencies. This process

can be automated using the SESTransient module which reruns the simulation until there are no more resonant frequencies that has not been included in the HIFREQ computation. A more detailed description of the HIFREQ computation method can be found in [26] and [27].

To achieve a reliable result, the conductors are split into segments that are shorter than $\lambda/6$ where λ is the shortest wavelength in the surrounding medium. The wavelength in air can be calculated as

$$\lambda_{air} = \frac{3 \cdot 10^8}{f}, \tag{4.1}$$

and in soil as

$$\lambda_{soil} = 3160\sqrt{\frac{\rho}{f}}, \tag{4.2}$$

where ρ is the soil resistivity and f the largest frequency used by FFTSES [28]. As the FFT assumes that the excitation signal is periodic, the initial value of the station GPR will not be zero if the duration of the simulation is not long enough to allow the signal to approach zero. However, using a longer simulation time increases the computation time if the sampling time is kept constant. Therefore, a simulation time of 2000 μs was used to compromise between computation time and keeping the final value low. Any deviation from an initial value of zero was removed in post processing of the result.

4.1.1 Cable route and grounding grid

A grounding grid was constructed in HIFREQ based on blueprints of a VSC-HVDC station provided by ABB Power Grids, HVDC. The resulting grid, cable trench, mast and rod of the station is shown in Figure 4.1.

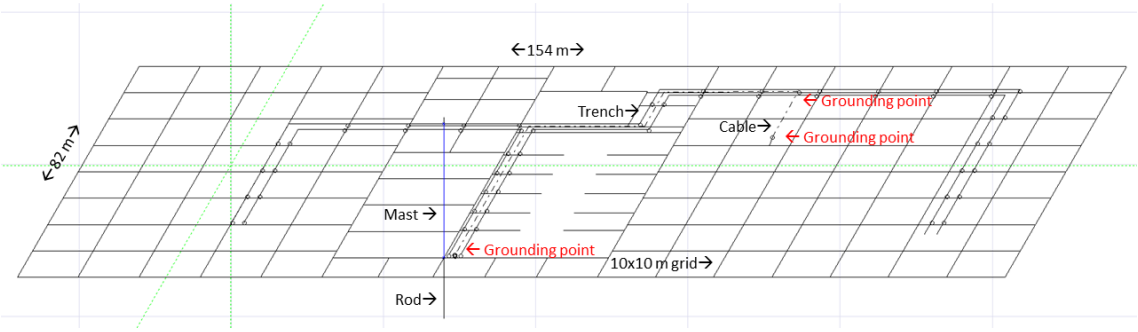

Figure 4.1: The layout used for the HIFREQ simulations.

Most of the grounding grid consisted of 10x10 m meshes. But certain areas, like under transformers, reactors and cooling towers, had no grid. The grounding grid

consisted of bare conductors buried in the soil at a depth of 1 m. The cable trench was located at a depth of 0.5 m with a width of 2 m. The mast and grounding rod located closest to a cable termination point was included in the model and will be used as the lightning strike point. The grounding points marked in the figure indicates the points where the cable screens were grounded. One PEC was placed on each side of the cable trench in the soil. A PEC and cable ladder was also added to the trench for the cases where mitigation methods were evaluated. The model of the cable trench in HIFREQ, with and without mitigation, is shown in Figure 4.2

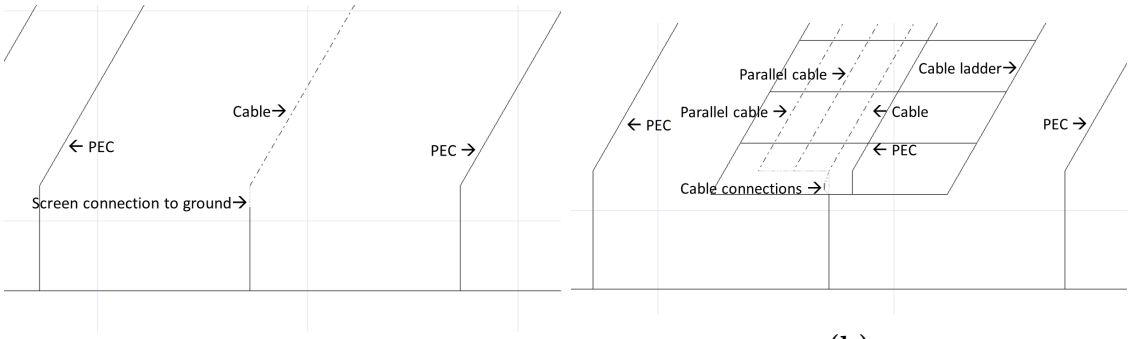

(a) **(b)**

Figure 4.2: Cable trench at the mast termination without mitigation (a) and with mitigation (b).

Another mitigation method under evaluation was moving the connection point between the mast and the grounding grid to the other side of the transformer wall. Which moves the injection point of the lightning current to the grid away from the cable trench. The effect of having the lightning current flow in a separate cable, isolated from the mast was also investigated. These two mast configurations are shown in Figure 4.3.

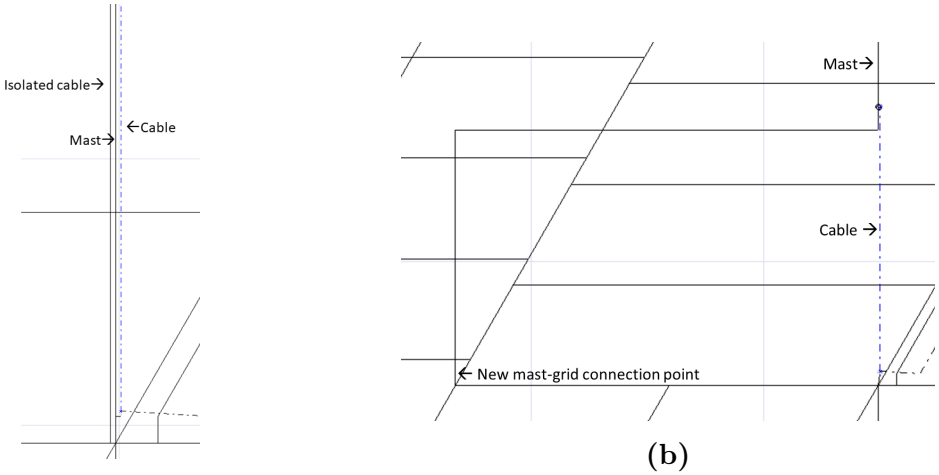

(a) **(b)**

Figure 4.3: Mast configuration with an isolated mast (a) and moving the mast-grid connection point (b).

The lightning mast had a height of 22 m and the grounding rod under the tower extends to a depth of 10 m. The dimensions of the conductors and material parameters are shown in Table 4.1.

Table 4.1: Dimensions of conductors and material parameters. Note that p.u is the per unit resistivity with copper as reference.

	Material	Resistivity	Permittivity	Permeability	Area [mm^2]
Grid	Copper	1 p.u	ϵ_0	μ_0	120
PEC	Copper	1 p.u	ϵ_0	μ_0	120
Ladder	Steel	17 p.u	ϵ_0	$300{\cdot}\mu_0$	314
Mast	Steel	17 p.u	ϵ_0	$300{\cdot}\mu_0$	314
Rod	Steel	17 p.u	ϵ_0	$300{\cdot}\mu_0$	314
Cable core	Copper	1 p.u	ϵ_0	μ_0	-
Cable screen	Copper	1 p.u	ϵ_0	μ_0	-
Insulation	PE	10^{20} Ω·m	$2.3{\cdot}\epsilon_0$	μ_0	-
	XLPE	10^{20} Ω·m	$2.3{\cdot}\epsilon_0$	μ_0	-
Soil	-	1500 Ω·m	$4{\cdot}\epsilon_0$	μ_0	-
Air	-	$2{\cdot}10^{16}$ Ω·m	ϵ_0	μ_0	-

The soil parameters were chosen to simulate a very dry soil with high resistivity and low permitivity which is the worst case for a station placed in a region with soil. The cable was routed from the control room and terminates next to the lightning mast. The dimensions and insulation type used for the different cables are presented in Table 4.2

Table 4.2: Cable dimensions and insulation. The first number in the core area row refers to the number of core conductors.

	Simplified	Signal	Power	CT	Lighting
Core area [mm^2]	1·21	14·1.5	4·16	2·2.5	3·2.5
Screen area [mm^2]	1.5	1.5	16	2.5	2.5
Jacket thickness [mm]	1	1	1	1	1
Total diameter [mm]	17	17	22.3	11.3	11.5
Insulation	PE	PE	XLPE	PE	PE

To include the effects of a cable trench, all cables and conductors located in the cable trench had a cylindrical air volume surrounding them. The simplified cable had 5 cm of air between the jacket and the soil. However, it was not possible to have multiple outer insulation layers for the cables with multiple conductors in HIFREQ and thus they only had an air layer of 6 cm between the screen and the soil. Other bare conductors in the trench had 3 cm of air surrounding them. A cross section of the different cable types, showing the orientation of the inner conductors are shown in Figure 4.4.

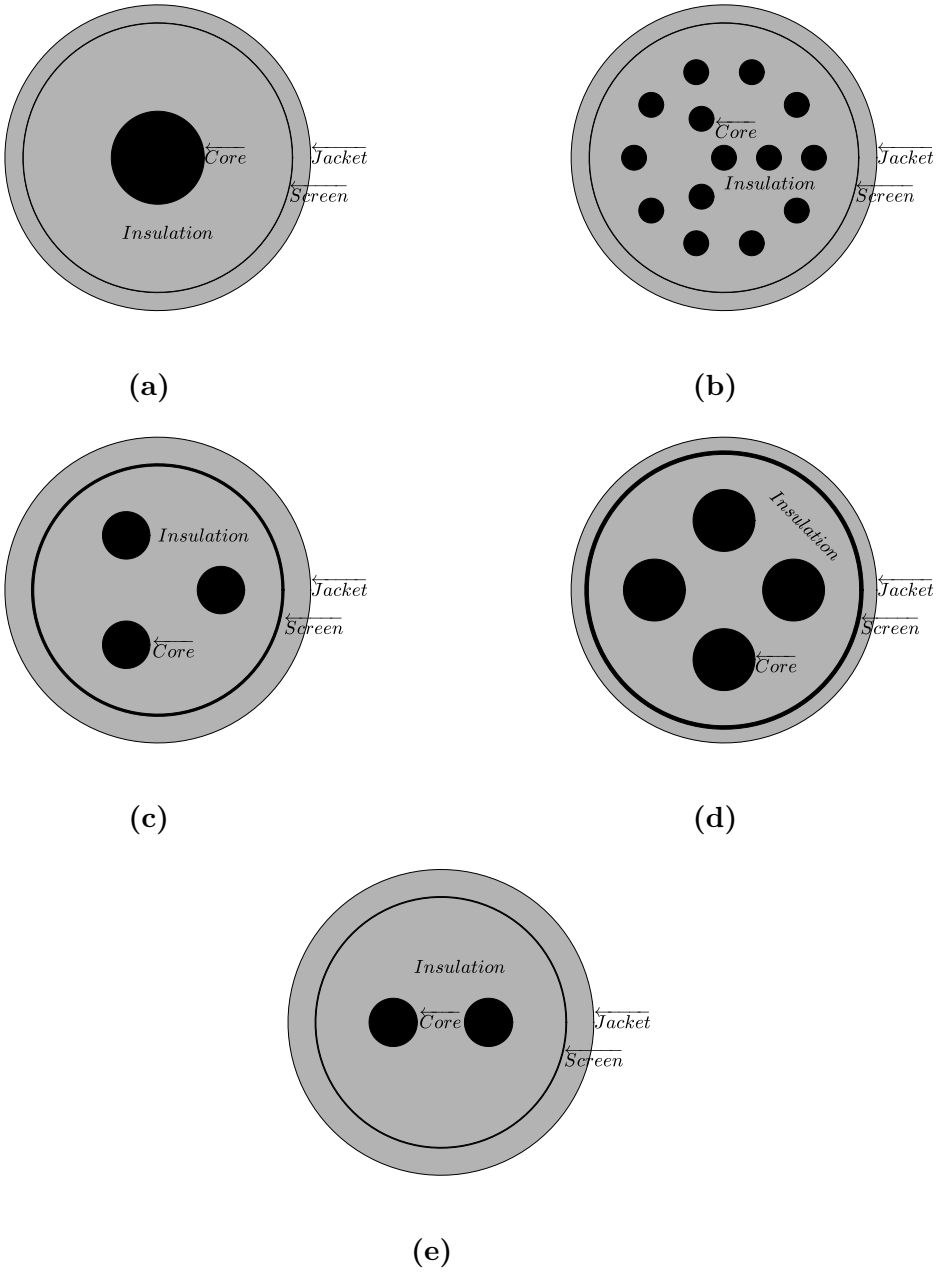

Figure 4.4: Cross section of the simplified signal cable (a), signal cable (b), lighting cable (c), power cable (d) and CT cable (e).

4.1.2 Lightning impulse wave shape

The Heildler function, described in chapter 3, was used to obtain an impulse shape shape of 1/200 μs as recommended by IEC for negative downward lightning. To get this waveshape, the constants were set to τ_1=1.82 μs and τ_2=285 μs. A peak current of 1 kA was used to obtain a result that can easily be scaled up to any desired peak current.

4.1.3 Simplified cable

The simplified cable was used to investigate the impact different mitigation methods and environmental factors. The base case consisted of only one cable and each change was introduced individually to illustrate its effect. First the effect of changing environmental parameters, such as soil resistivity and lightning current front time was looked. Note that the environmental parameters can not be changed for a given station and they only depend on the location of the station. The effect of including the frequency dependency of soil resistivity, using equation 2.3a was also investigated. After this, the effect of the different mitigation methods were looked at. The cases that will be investigated are summarised as:

1. Only signal cable.
2. Decrease soil resistivity to $150\,\Omega\,\mathrm{m}$.
3. Increase soil resistivity to $15\,000\,\Omega\,\mathrm{m}$.
4. Include soil resistivity frequency dependency.
5. Increase front time to $10\,\mu\mathrm{s}$.
6. Add PEC 0.1 m next to cable.
7. Add cable ladder 0.1 m below cable.
8. Move mast connection point to other side of transformer wall.

The results for the simplified cable can be found in section 5.1.

4.1.4 Cables terminating under the mast

The power, signal and CT cable terminated under the mast. The cable screens of these cables were connected to the grounding grid under the mast, at the control room wall and inside the control room. The results for the cables terminating under the mast are shown in section 5.2.

4.1.4.1 Power cable

The power cable was connected to a transformer in the control room in one end. The other end terminated at the bottom of the mast where it supplied a load. The circuit schematic of the cable connections is shown in Figure 4.5.

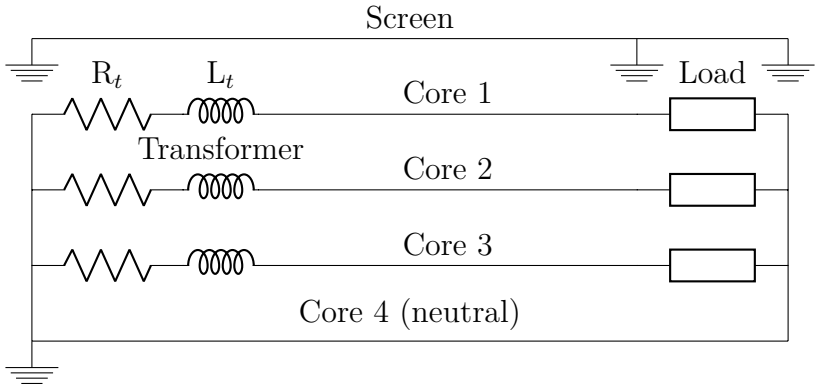

Figure 4.5: Equivalent circuit of the power cable connections.

The transformer had a Y connection on the low voltage side and the loads were assumed to be Y connected as well. The magnetizing inductance of the transformer and the grid impedance was neglected to simplify the transformer equivalent circuit. The neutral conductor was grounded (connected to the grounding grid) at the transformer. Three different load terminations were examined:

1. Motor (HV transformer cooling fan).
2. Heater (resistive heating element).
3. Open circuit (load switched off).

The resistance and inductance of the terminations and transformer is shown in Table 4.3

Table 4.3: Termination inductance and resistance per phase for the power cable.

	Resistance [Ω/phase]	Inductance [H/phase]
Transformer	$0.66 \cdot 10^{-3}$	$19.4 \cdot 10^{-6}$
Motor	74	0.22
Heater	$2.7 \cdot 10^{3}$	-

The transformer and cooling fan were assumed to be a combination of an inductance in series with a resistance. The heating element was purely resistive.

4.1.4.2 Signal cable

The signal cable used two conductors per signal and had a total of 14 conductors. In the control room the cable was terminated with a digital measurement card connected between each pair or inner conductors. The impedance of the card was assumed to be infinite. The cable was terminated with a digital sensor between each conductor pair which was also seen as an infinite impedance. The inner conductors were not grounded. The circuit schematic of the connections for one inner conductor pair is shown in Figure 4.6

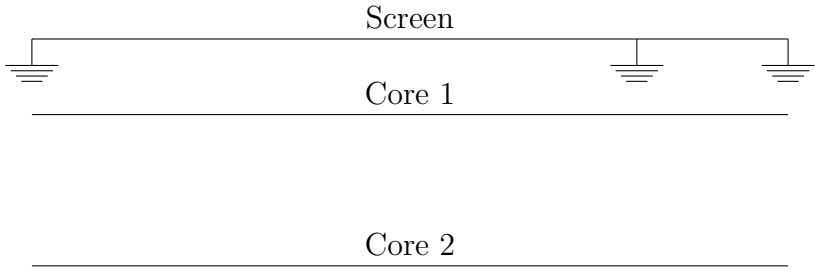

Figure 4.6: Equivalent circuit of the signal cable connections.

4.1.4.3 CT cable

The CT cable was connected to an analog measurement card at the termination in the control room. As the card is used to measure current (voltage drop over a small, known resistance), it was modelled as a short circuit. The termination at the other end was connected to the CT and as CTs are connected to HV lines in series, the

impedance on the high voltage side was neglected. The CT was instead modelled as a series combination of the magnetizing inductance and the winding resistance with values of L=188 H and R=5 Ω. The neutral conductor was grounded at the mast termination. The circuit schematic of the cable connections is shown in Figure 4.7

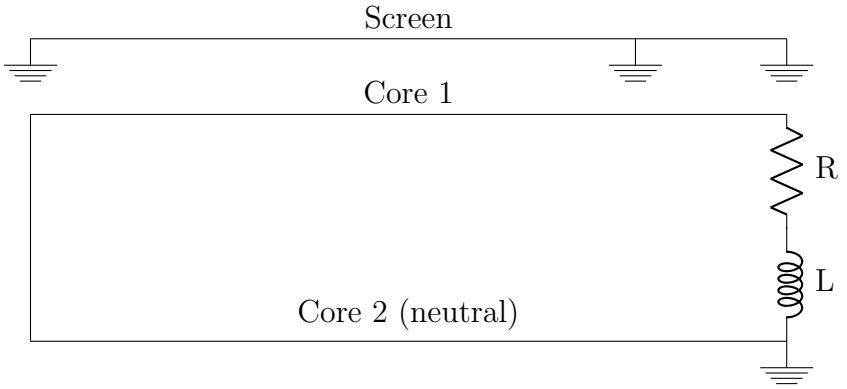

Figure 4.7: Equivalent circuit of the CT cable connections.

4.1.5 Mitigation

After the power, signal and CT cable were evaluated, the cable which experience the highest voltage stress was further simulated with added mitigation methods. This was done to demonstrate the effectiveness of the mitigation methods of the worst case and to investigate if the risk of breakdown could be reduced. The mitigation methods that were evaluated are:

1. PEC.
2. PEC and ladder.
3. PEC, ladder and moving mast-grid connection point.

The effectiveness of the mitigation methods on the cable with the highest voltage disturbance is shown in section 5.2.4.

4.1.6 Lighting cable

The path of the lighting cable differed from the other cables as it was not terminated under the mast. Instead it was routed up the mast and terminated 12 meters above the ground. The screen was also grounded where the cable terminates at the mast, in addition to the three grounding points used by the other cables. At the control room, the cable was terminated at the transformer. The other end was terminated by an LED light which was modelled as an open circuit. The circuit schematic of the cable connections is shown in Figure 4.8

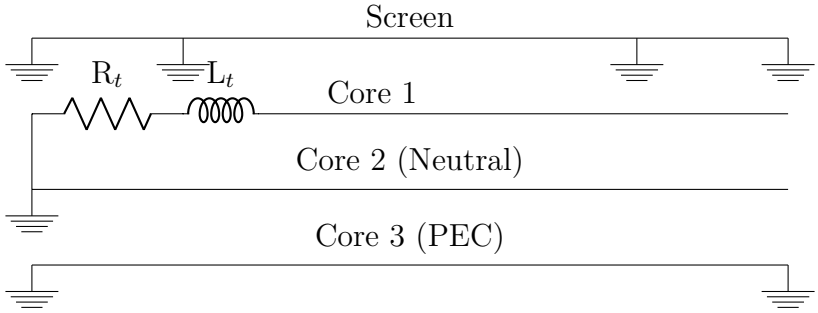

Figure 4.8: Equivalent circuit of the lighting cable connections.

The third conductor was used as an internal PEC which is connected to the grounding grid at the two cable terminations. The mitigation methods that were evaluated for the lighting cable are:

1. PEC and cable ladder in the cable trench.
2. PEC on the mast.
3. Move mast-grid connection point.
4. Isolate mast from the lightning current with a separate cable.
5. Enclose the lighting cable in a copper pipe.

A cable with multiple core conductors could not be used with a second screen (copper pipe) in HIFREQ. However, it was possible to add a second screen if only one core conductor was used. Therefore, the case with a copper pipe used a simplified lighting cable with one equivalent core conductor, floating at both cable termination points. The copper pipe had an inner radius of 1 cm and an outer radius of 1.3 cm.

As the lighting cable screen was grounded very close to the mast striking point, a high current was expected to flow in the screen during the lightning strike. Therefore, the screen current was also examined and the temperature increase of the cable was calculated for the different cases. The resulting voltage disturbance for the lighting cable can be found in section 5.3. The resulting screen current and temperature increase is shown in section 5.4.

4.1.7 Risk analysis

The risk analysis was conducted in Matlab using the rolling sphere method described in section 3.1.2. The lightning current was assumed to be log normal distributed with a median value of 31.1 kA and logarithmic standard deviation of 0.484. The minimum current that causes damage was obtained from the simulations in HIFREQ. To account for different geographical regions, three different number of thunderstorm days/year was investigated: 10, 20 and 30 days/year. These numbers will encapsulate the number of thunderstorm days/year typically seen across Europe. Note that the number of thunderstorm days/year can be significantly higher closer to the equator.

4.2 Simulink

4.2.1 Equivalent circuit

The result from the simplified signal cable was compared with an equivalent circuit simulation of the cable to investigate the effect which causes the cable voltage disturbance. The equivalent cable parameters were calculated according to section 2.2.3. Simulink was used to simulate the equivalent circuit and the screen current was imported from the case simulated with the simplified signal cable. The cable was split into the same number of segments used in HIFREQ, each consisted of an equivalent circuit according to Figure 4.9.

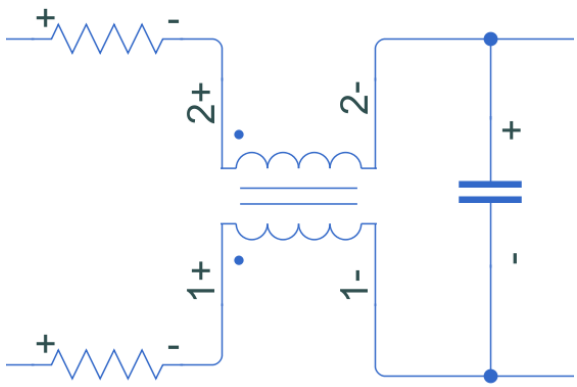

Figure 4.9: One segment of the equivalent circuit used in Simulink.

As frequency dependant parameters could not be used in Simulink, the resistance was calculated at a single frequency. The front time of the lightning current was 1 μs and therefore the maximum frequency content of the impulse was in the MHz range. The resistance was calculated at 400 kHz to use a value that was in between the maximum and lower frequencies. The inductance was calculated using equation 2.8 assuming that all current flows at the edge of the conductor (neglecting the internal inductance). The comparison between the Simulink and HIFREQ result is shown in section 5.1.3.

4.3 Comsol

4.3.1 Breakdown voltage of LV cables

An electrostatic 2D Comsol simulation was used to determine the electric field in the different LV cables. Comsol is based on the finite element method in which the geometry is split into small segments and differential equations are solved for each segment. When using the electrostatic physics, charge conservation is applied to the domain under consideration. This uses Gauss' law and the gradient of the potential,

$$\nabla \cdot \mathbf{D} = \rho_v \qquad -\nabla V = \mathbf{E}, \tag{4.3}$$

to obtain the differential equations used to calculate the electric field for the geometry. The cables were constructed according to Figure 4.4 and an extremely fine mash was used to get an accurate result. All inner conductor boundaries were assigned the same potential of 1 kV and the screen was grounded. As mentioned in section 2.2.2, the dielectric strength of PE and XLPE insulation is 35-50 kV/mm. To get a conservative result, the applied potential was scaled to get a maximum electric field of 30 kV/mm and the scaled potential was seen as the rated impulse voltage of the cable. The result from the Comsol simulations can be found in section 5.5.

5

Simulation results and analysis

5.1 Simplified cable

The highest voltage disturbance of the simplified signal cable appears at the two cable terminations and is shown in Figure 5.1

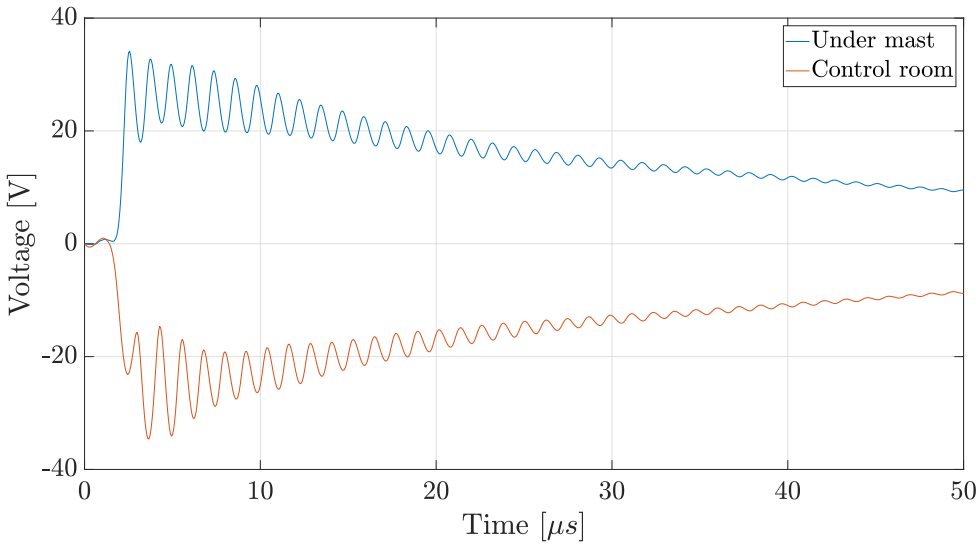

Figure 5.1: Core to screen voltage disturbance for the simplified signal cable.

The voltage at the two ends are almost identical but of opposite sign and there are some damped oscillations with a frequency around 1 MHz. For the remaining simplified signal cases, only the voltage disturbance under the mast will be examined as the magnitude is similar.

5.1.1 Effect of changing environmental parameters

The environmental parameters that were examined was soil resistivity, frequency dependency of soil resistivity and lightning current front time. The effect of changing the soil resistivity on core to screen voltage, GPD between grounding points and screen current is shown in Figure 5.2

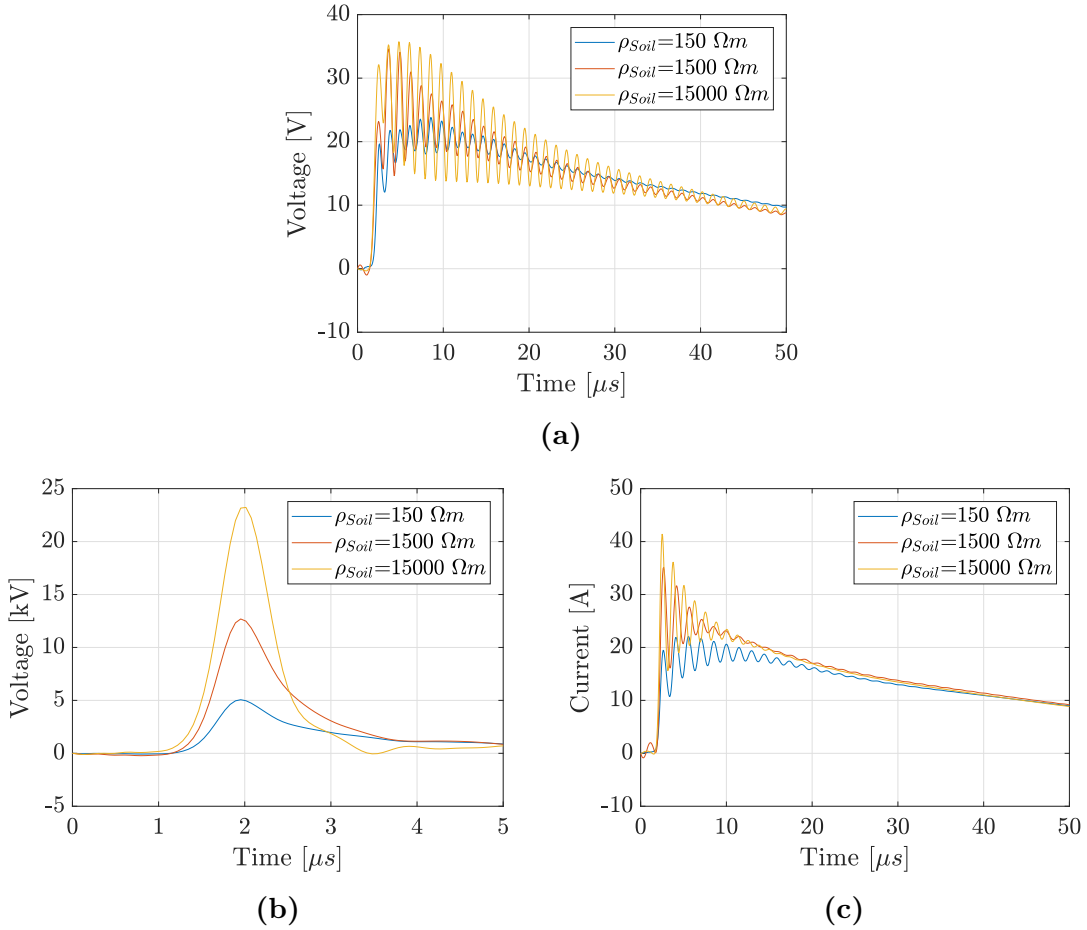

Figure 5.2: The effect of increasing soil resistivity from 150 Ωm to 15000 Ωm on the screen to core voltage disturbance (a), GPD between grounding points (b) and screen current (c).

The GPD between grounding points increase as the soil resistivity is increased. The higher GPD results in a higher screen current as the soil resistivity increase. A coupling between the screen current and screen to core voltage can be observed as the screen to core voltage also increase with increasing soil resistivity. The effect of including frequency dependency of the soil resistivity and increasing the front time of the lightning current is shown in Figure 5.3

Including the frequency dependency of soil resistivity decreases the GPD between the grounding points as the resistivity is lower for the higher frequencies and more current will flow in the soil instead of the grounding grid. Similarly, when decreasing the front time results in a lower GPD as the frequency content of the lightning impulse is lower and thus also the impedance of the grounding grid. The lower GPD implies a lower screen current and also a lower screen to core voltage disturbance.

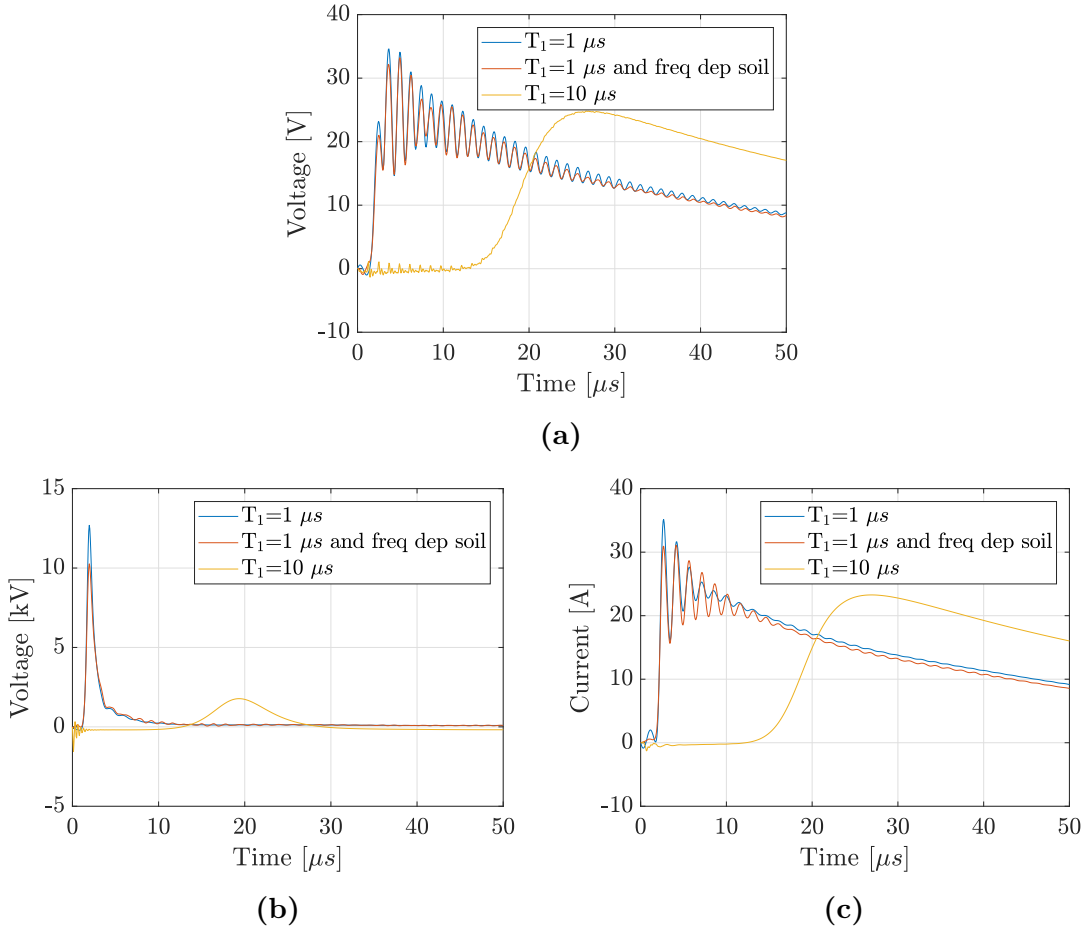

Figure 5.3: The effect of including the frequency dependency of soil resistivity and increasing the lightning current front time on the screen to core voltage disturbance (a), GPD between grounding points (b) and screen current (c).

5.1.2 Evaluation of mitigation methods

The mitigation methods were evaluated one by one to see the individual effects of each mitigation method. The voltage disturbance when adding a PEC, cable ladder and moving the connection point between the mast and the grounding grid to the other side of the wall is shown in Figure 5.4.

Both the PEC and cable ladder decrease the voltage disturbance. The PEC seem to be more effective and it reduces the voltage from 35 V to 18 V. Moving the injection point reduces the peak voltage disturbance to 20 V.

5.1.3 Equivalent circuit evaluation

A comparison between the signal cable base case and the simulated circuit voltage disturbance can be seen in Figure 5.5.

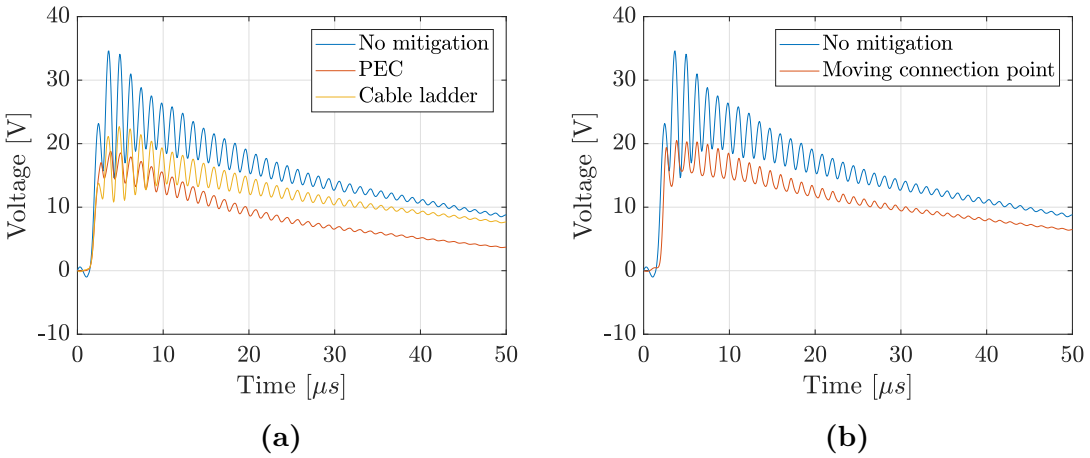

(a) **(b)**

Figure 5.4: Core to screen voltage disturbance at the termination under the mast for the simplified signal cable, with PEC and with cable ladder (a) and when moving the injection point (b).

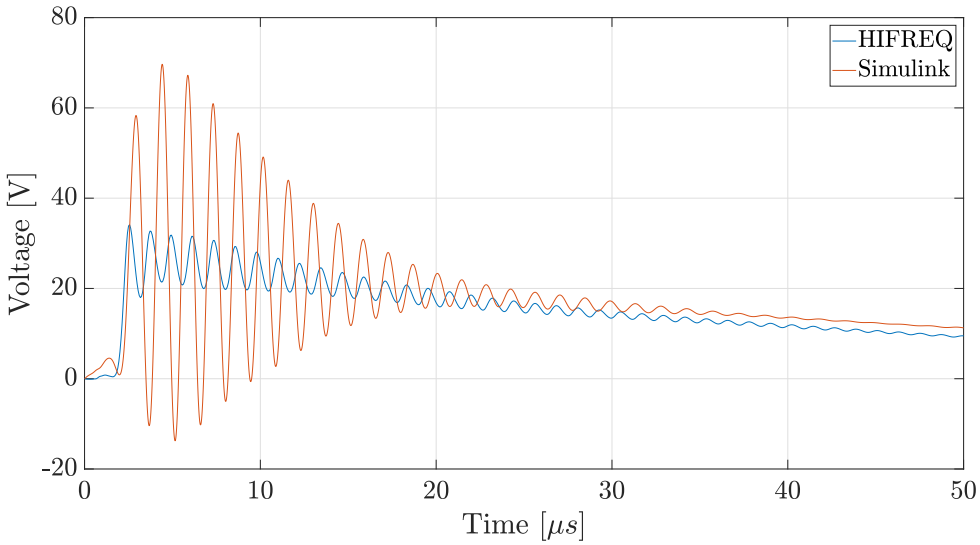

Figure 5.5: Core to screen voltage disturbance at the termination under the mast for the simplified signal cable and the disturbance obtained from the equivalent circuit simulation in Simulink.

The magnitude of the oscillation is much higher in the Simulink simulations and there seem to be less damping. But the frequency of the oscillation and wave shape is similar. The reason for the lower damping (and higher magnitude) might be that Simulink can not account for the increase in resistance for the high frequency oscillations caused by the skin effect. Having a higher resistance for the high frequency oscillations would cause the magnitude to decrease as can be observed in the HIFREQ simulations. However, from the Simulink simulations it can be seen that the voltage disturbance seen in HIFREQ can be reproduced by using the screen current and an equivalent circuit of the cable. Indicating that screen current to voltage coupling is the mechanism behind the voltage disturbance.

5.2 Cables terminating under mast

5.2.1 Power cable

The power cable was simulated with three different types of loads. The neutral conductor at the termination point under the mast was found to experience the highest voltage disturbance in all cases. The resulting voltage disturbance at the termination point under the mast, between the neutral conductor and screen for the respective loads is shown in Figure 5.6.

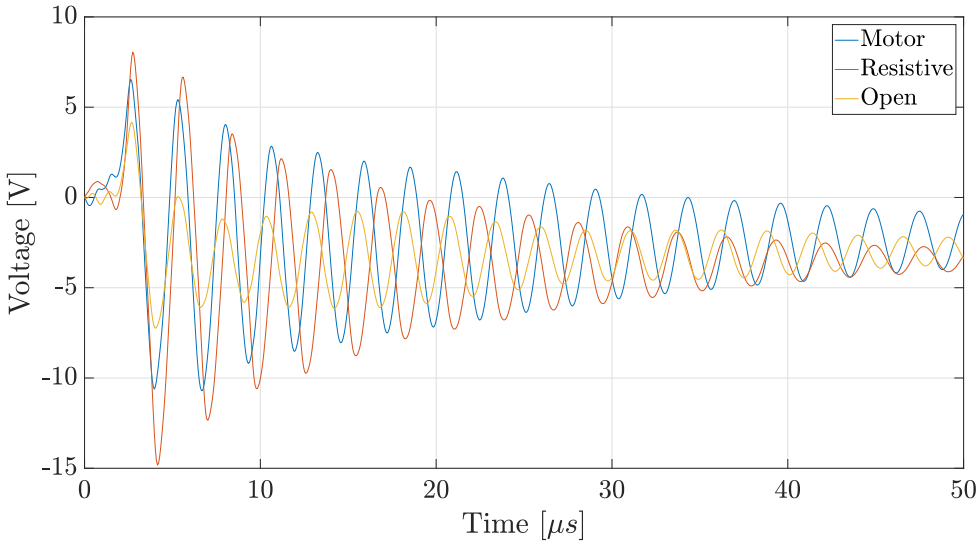

Figure 5.6: Core to screen voltage disturbance for the power cable with different load terminations.

The case with resistive termination experiences the highest voltage peak with a value of -15 V. Some damped oscillations with a frequency of about 200 kHz can be observed in all cases.

5.2.2 Signal cable

For the signal cable, the highest voltage disturbance between the core conductors and the screen was found at the cable termination in the control room. The voltage disturbance for the three different core conductor layers is shown in Figure 5.7.

The voltage disturbance at the two ends is almost identical but of opposite sign with a peak value of 40 V. For the inner and middle layer the disturbance is slightly increased. For all layers some damped oscillations can be observed with a frequency of approximately 1 MHz.

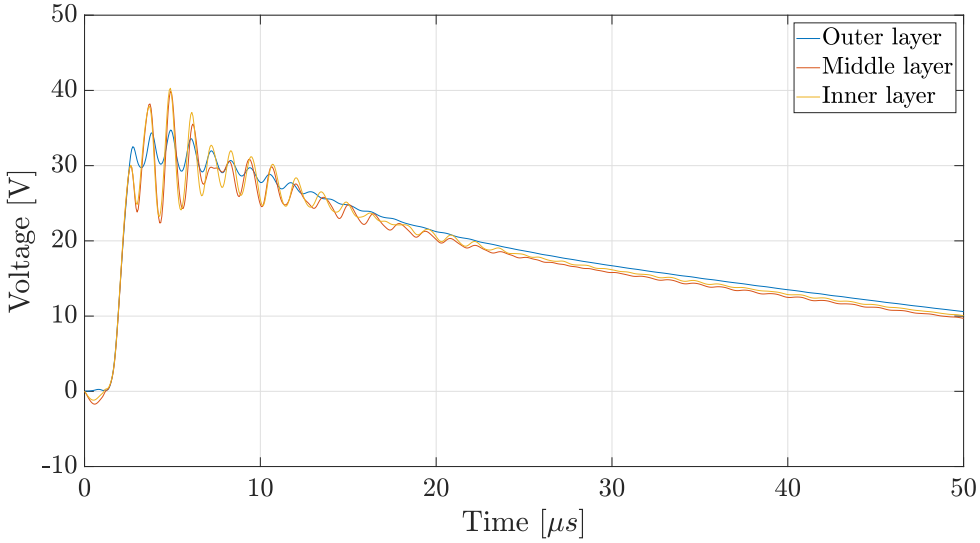

Figure 5.7: Core to screen voltage disturbance for the 3 different conductor layers of the signal cable.

5.2.3 CT cable

The highest voltage disturbance between the core conductors and the screen occurred at the termination under the mast for the CT cable. The voltage disturbance is shown in Figure 5.8.

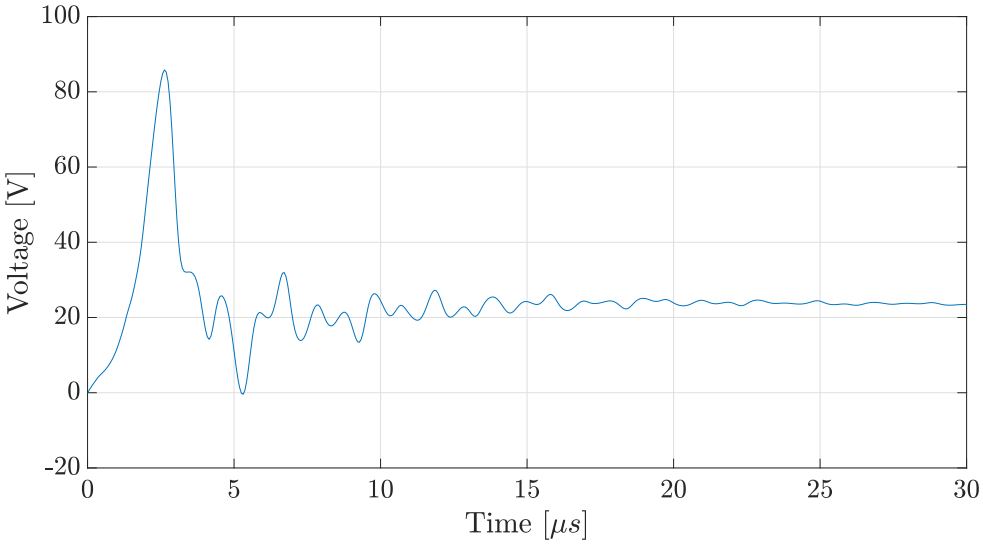

Figure 5.8: Core to screen voltage disturbance for the CT cable.

The peak disturbance is about 83 V and damped oscillations of multiple frequencies are observed.

5.2.4 Worst case mitigation

The peak magnitude of the voltage disturbance per kA of lightning current for the cables terminating under the mast is shown in Figure 5.9

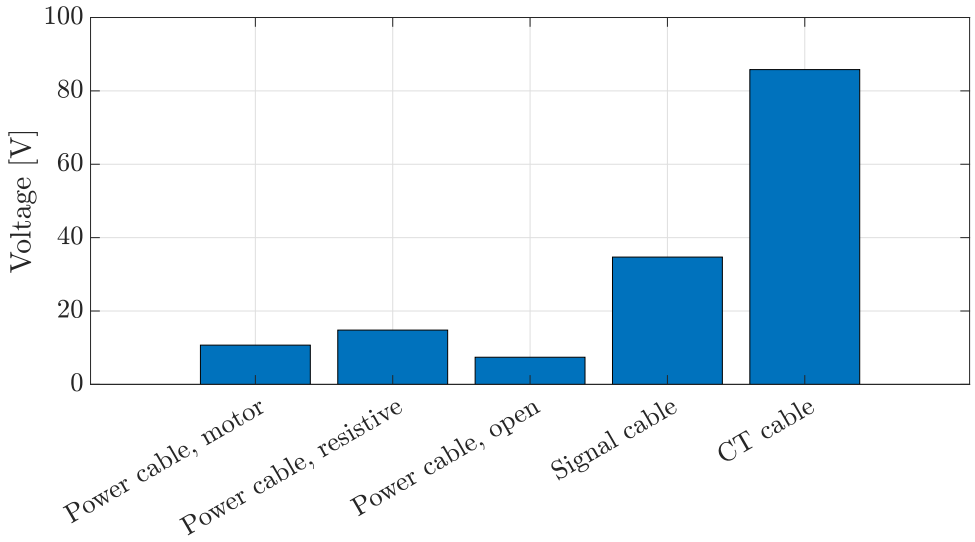

Figure 5.9: Peak voltage disturbance per kA of injected current for the cases without mitigation.

The CT cable experiences the highest voltage disturbance and thus it will be used to investigate the effectiveness of the mitigation methods. The voltage disturbance between the core and screen when adding a PEC, PEC and cable ladder and when moving the connection between the mast and the grounding grid as well is shown in Figure 5.10

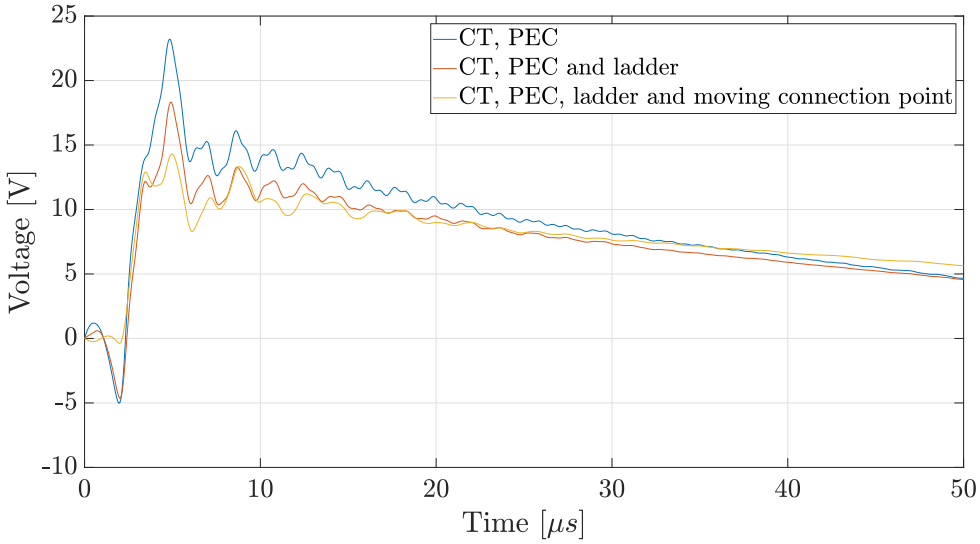

Figure 5.10: Core to screen voltage disturbance for the CT cable when adding mitigation.

The voltage disturbance is reduced from a peak value of 83 V to 23 V when adding a PEC. Using a PEC and cable ladder further reduces the peak disturbance to 18 V and also moving the injection point results in a peak of 14 V.

5.3 Lighting cable

The voltage disturbance to the lighting cable was the highest at the grounding point on the mast. The voltage disturbance when having the lightning current flow through the mast and when it flows in a separate insulated cable is shown in Figure 5.11.

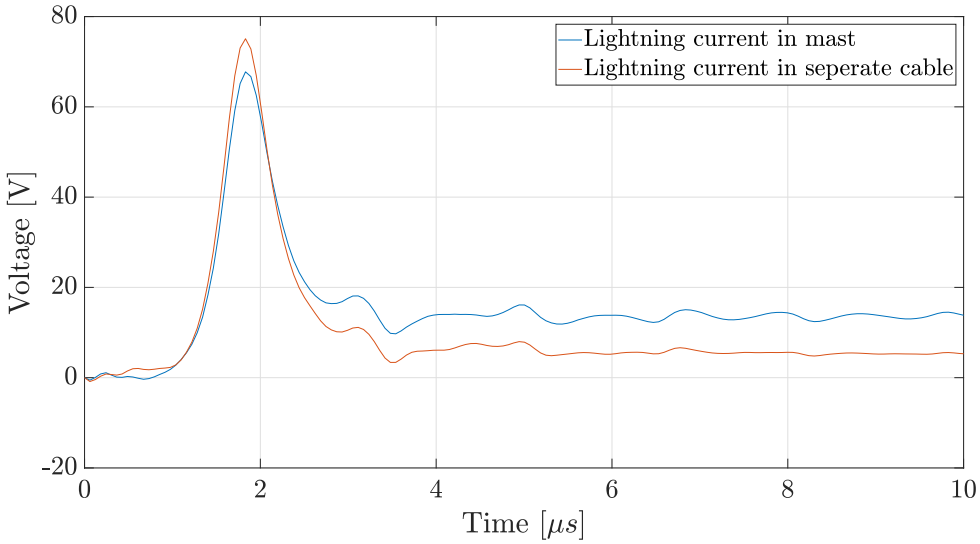

Figure 5.11: Core to screen voltage for the lighting cable with different mast configuration.

Having the lightning current flow the mast results in a peak voltage disturbance of 67 V. Having the lightning current flow in a separate insulated cable increases the disturbance to 75 V.

5.3.1 Lighting cable mitigation

The mitigation methods investigated for the lighting cable were:

1. Adding a PEC and cable ladder on the under ground part of the cable (Current in mast).
2. Moving the injection point (Current in mast).
3. Adding a PEC on the mast (with current in separate isolated cable).
4. Adding a copper pipe to the cable (simplified lighting cable with current in separate isolated cable).

It was not possible to add an extra screen to a cable with multiple inner conductors in HIFREQ. In this case, the lighting cable was instead simulated with with one equivalent core conductor (floating in both ends). The core to screen voltage disturbance for the different mitigation methods is shown in Figure 5.12.

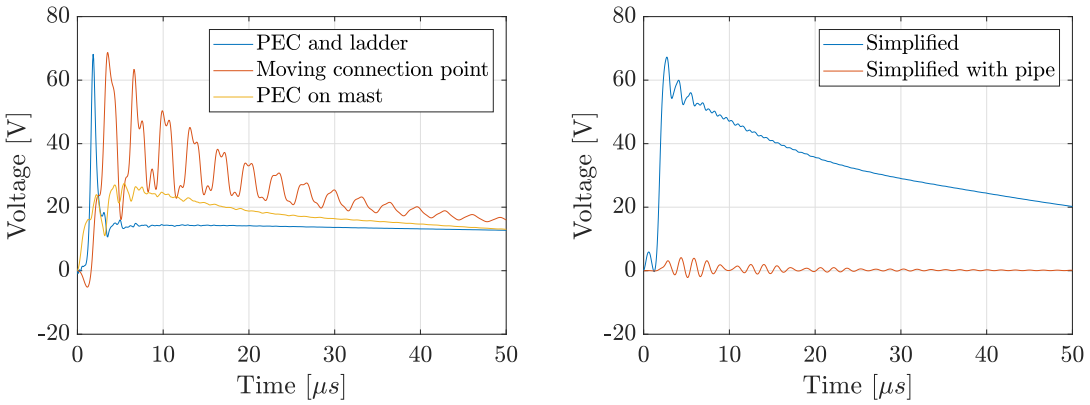

(a) **(b)**

Figure 5.12: Core to screen voltage for the lighting cable (a) and simplified lighting cable (b) when adding mitigation.

Adding a PEC and cable ladder in the ground does not affect the voltage disturbance at the top of the mast. Moving the injection point increases oscillations in the disturbance, however the peak is not affected significantly. Having a PEC next to the part of the cable that goes up the mast reduces the disturbance from 75 V to 25 V. The copper pipe mitigates the induced voltage disturbance to below 5 V.

5.4 Overheating of cable screens

The lighting cable had the highest current flowing in the screen as it was grounded both at the middle and bottom of the mast. The screen current for the base case and the effect of adding mitigation methods is shown in in Figure 5.13

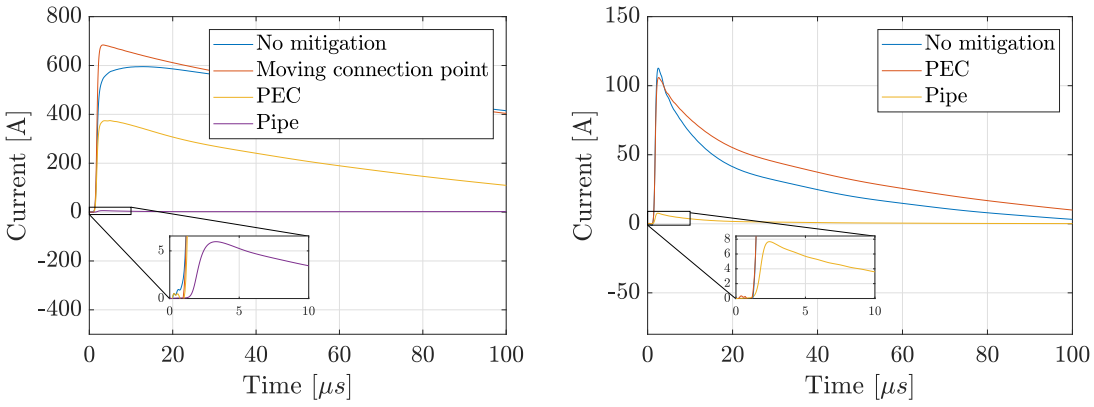

(a) **(b)**

Figure 5.13: Screen current in the lighting cable when adding mitigation methods with lightning current in the mast (a) and in a separate cable (b). Note that there is a difference in y-axis scaling between (a) and (b).

The screen current is the the highest for the case with the injection point moved to the other side of the transformer wall. This is expected as the inductance of the mast is increased. The case with regular mast termination also result in a high screen current of about 600 A peak. Having the lightning current flow in a separate cable isolated form the mast significantly decreases the screen current disturbance to a peak of around 100 A. Adding a PEC further mitigates the lightning current and the pipe reduces it to only a few amps. The lighting cable was insulated with PE, being able to withstand a temperature of 130 °C for short a duration [17]. If an operating temperature of 50 °C is assumed, the temperature increase during a lightning strike should not exceed 80 °C. The temperature increase of the cable screens for a 100 kA stroke and the current needed to get a temperature increase of 80 °C were calculated using equation 2.11. The result for the different cases is shown in Table 5.1.

Table 5.1: Temperature increase of the cable screen for a lightning strike of 100 kA and the current to get a temperature increase of 80 °C for different mast configurations.

Case	$\Delta\theta$ [°C] at 100 kA	I to get $\Delta\theta$=80 °C [kA]
Current in mast	766	44.35
Moving injection point	786	44.04
Current in separate cable	1.25	-
Strike to separate cable and pipe	0.006	-
Separate cable and PEC	2.28	-
Strike to mast and PEC	81.3	99.29
Strike to mast and pipe	0.033	-

The cases having the lightning current flow in a separate isolated cable will not result in a significant increase in the lighting cable temperature. The same can be observed when adding a copper pipe as the temperature increase is minimal. However, all cases having the lightning current in the mast and not using a pipe will result in a high screen current and temperature increase.

5.5 Rated impulse voltage of LV cables

The voltage between the screen and core needed to get a maximum electric field of 30 kV/mm (seen as the rated cable impulse voltage) for the different cables is shown in Table 5.2.

Table 5.2: Core to screen voltage needed to get a maximum electric field of 30 kV/mm.

Cable	Rated voltage [kV]
Power	54
Signal	43
CT	33
Lighting	27

The calculated rated impulse voltage is significantly higher than the rated continuous voltage specified in the cable data sheets. This could be since cable manufactures want to keep a safety margin and take into account that cable ageing might affect the characteristics of the insulation material.

5.6 Risk analysis

From section 5.2 and 5.3 it can be concluded that the highest voltage disturbance per kA of lightning current was below 90 V. As the rated impulse voltage was calculated to above 25 kV for all cables, the lightning current needed to get a cable fault cause by a voltage disturbance would be above 270 kA. The risk of this is very low and according to the risk calculation model there would be millions of years between lightning strikes of this magnitude, even when considering stations placed in a region with 30 thunderstorm days/year. Therefore, overvoltages in LV cables does not need to be considered when doing lightning risk calculations and having the cables close to the lightning mast does not result in a disturbance high enough to damage the cable.

The risk of overheating the cable screen is the only risk and it can be solved by using mitigation methods. The result in section 5.4 shows that the temperature increase for the cases having an isolated mast or a copper pipe surrounding the cable gives negligible temperature increases. Only the cases with lightning current in the mast result in a screen current that can potentially damage the cable and only these cases were considered in the risk calculations. The number of years between strikes to the mast exceeding the currents specified in the third column of Table 5.1 is shown in Table 5.3 for different number of thunderstorm days/year.

Table 5.3: Time between strikes that will cause a fault for different cases.

Case	Thunderstorm days/year	Time between faults [yr]
No mitigation	10	348
	20	146
	30	88
PEC on mast	10	6125
	20	2575
	30	1551
Moving mast connection	10	342
	20	144
	30	87

Moving the mast-grid connection point slightly decreases the time between faults and adding a PEC to the mast significantly increases it. However, by using a copper pipe or isolating the mast, the risk can be removed completely.

5.7 Reliability of result for high currents

As discussed in section 2.1.1, soil can become ionised when subjected to an electric field above approximately 300-400 kV/m. This would increase the conductivity of the soil drastically and thus lower the cable disturbance. The magnitude of the electric field at the mast-grid connection point (where the highest electric field can be expected) is shown in Figure 5.14

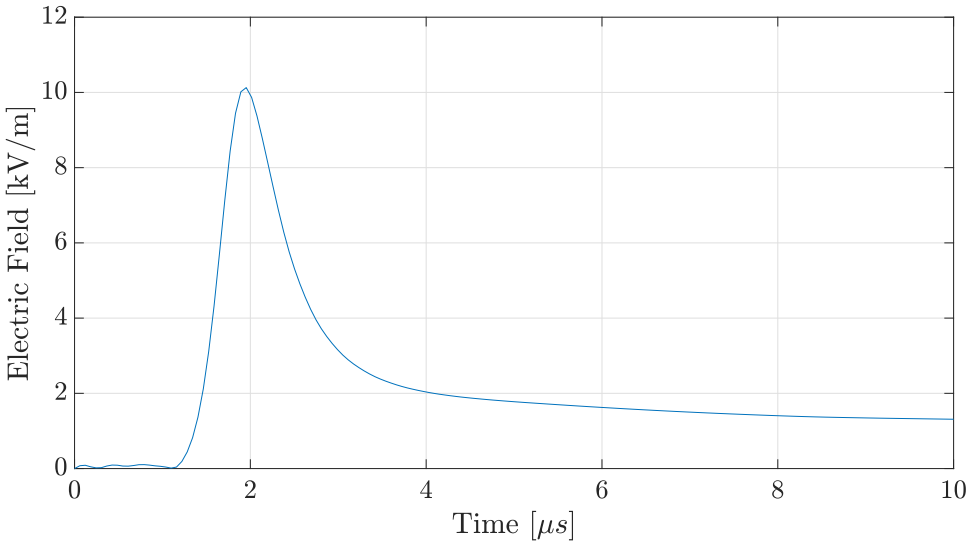

Figure 5.14: Electric field at the mast-grid connection point.

The maximum electric field is about 10 kV/m for 1 kA of lightning current, implying that soil ionisation can be expected at 30 kA if the lower range of the soil ionisation limit is used. As soil ionisation is not included in the simulations, the result will be more conservative at a current above 30 kA.

6
Conclusion

This thesis has investigated disturbances to different types of LV cables routed close to a lightning mast in a HVDC station. The cause and magnitude of the disturbance has been evaluated and mitigation methods have been tested using the HIFREQ simulation tool in CDEGS. A risk evaluation based on the rolling sphere method has also been conducted to evaluate the risk of a fault due to a strike to the examined mast.

It was shown that the reason for the disturbance to LV cables is the high GPD between cable screen grounding points created during a lightning strike when one grounding point is close to the mast. The GPD causes a current disturbance in the screen which is coupled to a core to screen voltage disturbance. The coupling mechanism is both capacitive, through the cable capacitance, and inductive through the mutual inductance between the screen and core. If the core and screen is connected through a load there is also a conductive coupling. The inductive and capacitive coupling could be reproduced using an equivalent circuit of the cable in Simulink.

The effect of changing environmental parameter and adding mitigation methods can be summarised as:

- Environmental factors
  - Increasing the soil resistivity increases the disturbance.
  - Including the frequency dependency of soil resistivity decreases the disturbance.
  - Increasing the lightning current front time decreases the disturbance.
- Mitigation methods
  - Adding a PEC and cable ladder under ground reduces the disturbance for all cables except for the lighting cable.
  - Moving the mast-grid connection point reduces the cable disturbance for all cables except the lighting cable.
  - Isolating the mast from the lightning current increases the lighting cable disturbance slightly.
  - Adding a PEC on the mast reduces the lighting cable disturbance.
  - Adding a copper pipe surrounding the lighting cable reduces the disturbance.

The risk analysis showed that the risk of lightning causing overvoltages in LV cables that result in damage is minimal and can be neglected. However, the main problem identified during a lightning strike was the heating of the lighting cable screen. It was shown that having an isolated mast or surrounding the lighting cable with a

copper pipe were the most viable options as this reduces the cable screen temperature increase to an insignificant number.

6.1 Further work

Some points that could be investigated to further build on the result are:

- Impact of including adjacent equipment on the number of strikes to the mast.
- Investigate the voltage and current ratings of the equipment connected to the different cables. This might have an impact the risk analysis.
- Some further mitigation methods that could be investigated for the lighting cable is to increase the screen area and use a XLPE insulated cable to increase the rated short circuit temperature.
- Investigate the impact of using other screen grounding methods, such as only grounding one end of the cable screen.

Bibliography

[1] ABB AB, "HVDC Light It's time to connect," ABB AB, Tech. Rep., 2017.

[2] G. Milne, "Ground voltage and current cancellation by co-axial cable." in *COMSIG*, Rondebosch, South Africa, Sep. 1998.

[3] *Protection against lightning – Part 1: General principles*, IEC 62305-1, Geneva, Switzerland, Dec. 2010.

[4] K. berger, R. Anderson, and H. Kröninger, "Parameters of lightning flashes," *Electra*, no. 41, pp. 23–37, 1975.

[5] N. Theethayi, "Electromagnetic interference in distributed outdoor electrical systems, with an emphasis on lightning interaction with electrified railway network," Ph.D. dissertation, Uppsala University, Uppsala, Sweden, Sep. 2005.

[6] L. GRCEV, "Transient Voltages Coupling to Shielded Cables Connected to Large Substation Earthing Systems Due to Lightning," in *CIGRÉ 1996 : 36-201*, Skopje, Macedonia, 1996.

[7] Working Group 01 of Study Committee 33, "Guide to procedures for estimating the lightning performance of transmission lines," CIGRÉ, Paris, France, Tech. Rep., Oct, 1991.

[8] *IEEE Guide for Safety in AC Substation Grounding*, IEEE Std 80, Substations Committee of the IEEE Power and Energy Society, New York, NY, USA, Dec. 2013.

[9] Working Group C4.33, "Impact of soil-parameter frequency dependence on the response of grounding electrodes and on the lightning performance of electrical systems," CIGRÉ, Tech. Rep., Oct. 2019.

[10] O. Gouda, G. Amer, and T. Elkhodragy, "Factors affecting transient response of grounding grid systems," in *SSD*, Aug. 2008.

[11] B. Zhang, J. He, J.-B. Lee, X. Cui, Z. Zhao, J. Zou, and S.-H. Chang, "Numerical analysis of transient performance of grounding systems considering soil ionization by coupling moment method with circuit theory," *IEEE Transactions on Magnetics*, vol. 41, no. 5, pp. 1440–1443, May 2005.

[12] A. M. Mousa, "The soil ionization gradient associated with discharge of high currents into concentrated electrodes," *IEEE Transactions on Power Delivery*, no. 9, pp. 1669–1677, 1994.

[13] Working Group C4.208, "EMC within Power Plants and Substations," CIGRÉ, Tech. Rep., Apr. 2013.

[14] H. W. Ott, *Electromagnetic Compatibility Engineering*. Hoboken, NJ, USA: Wiley, 2009.

[15] *Power cables with extruded insulation and their accessories for rated voltages from 1 kV (Um = 1,2 kV) up to 30 kV (Um = 36 kV) – Part 1: Cables for*

rated voltages of 1 kV (Um = 1,2 kV) and 3 kV (Um = 3,6 kV), IEC 60502-1, International Electrotechnical Commission, Nov. 2009.

[16] A. Küchler, *High Voltage Engineering*. Schweinfurt, Germany: Springer Vieweg, 2018.

[17] *Comparison among insulation materials*, Nexans, 2008.

[18] D. K. Cheng, *Field and Wave Electromagnetics*, 2nd ed. Chevy Chase, MD, USA: Pearson Education Limited, 2013.

[19] E. B. Rosa, *The Self and Mutual Inductances of Linear Conductors*. Washington, USA: U.S. Department of Commerce and Labor, Bureau of Standards, 1908.

[20] Working Group C4.407, "Lightning Parameters for Engineering Applications," CIGRÉ, Tech. Rep., Aug. 2013.

[21] CIGRÉ Working Group C4.407, "CIGRÉ Technical Brochure on Lightning Parameters for Engineering Applications," in *SIPDA*, Belo Horizonte, Brazil, Oct 2013, pp. 373–377.

[22] *IEEE Guide for Direct Lightning Stroke Shielding of Substations*, IEEE Std 998, Substations Committee of the IEEE Power and Energy Society, New York, NY, USA, Dec. 2012.

[23] R. Holle and W. Brooks., "Vaisala 2018 Annual Lightning Report," Vaisala, Tech. Rep., 2019.

[24] CIGRÉ Working Group C4.501, "Guideline for Numerical Electromagnetic Analysis Method and its Application to Surge Phenomena," CIGRÉ, Tech. Rep., Jun. 2013.

[25] S. Nikolovski, P. Maric, Z. Baus, and B. Stefic, "Computation of electromagnetic field of transformer station 110/10(20) kv using the cdegs software," in *EUROCON 2007 - The International Conference on Computer as a Tool*, Warsaw, Poland, Sep. 2007.

[26] F. P. Dawalibi and A. Selby, "Electromagnetic fields of energized conductors," *IEEE Transactions on Power Delivery*, vol. 8, no. 3, pp. 1275–1284, 1993.

[27] A. Selby and F. P. Dawalibi, "Determination of current distribution in energized conductors for the computation of electromagnetic fields," *IEEE Transactions on Power Delivery*, vol. 9, no. 2, pp. 1069–1078, 1994.

[28] SESTECH, *HOW TO... ENGINEERING GUIDE: Lightning Transient Study of a Communication Tower*, 16th ed., Quebéc, Canada, 2017.